IEEJ TRANSACTIONS ON ELECTRICAL AND ELECTRONIC ENGINEERING
IEEJ Trans 2019
Published online in Wiley Online Library (wileyonlinelibrary.com). DOI:10.1002/tee.23043

Paper

Ordered Clustering Method and Degradation Trend Analysis for Performance Degradation of Tantalum Capacitor

Jingying Zhao[a], Non-member
Jianmeng Liu, Non-member

The performance degradation trend of a tantalum capacitor has different characteristics in different degradation regimes with different temperatures and humidity. Clustering method and degradation trend analysis can be useful for early warning of life. In this paper, according to the degradation characteristics of the capacitance and the dissipation factor with different temperature and humidity, the experiment is designed, and the failure mechanisms of different degeneration regimes are analyzed. After the ordered clustering method is introduced, using the natural property and the change rate $\alpha(k)$ of the slope $\beta(k)$ of the error function $\delta[p(m,k)]$, the determination method of the optimization clustering number is put forward. The Davies-Bouldin Index is proposed as the evaluation method of the ordered clustering result, and the validation of the evaluation method was verified by the degradation data with other stresses. For the stable degradation regime, the degradation trend analysis is completed. The error result shows that the degradation fitting functions can be a good fit for the degradation trend with different stress. According to the degradation fitting analysis, the degradation prediction method is described to find the relationship between prediction life and different temperature and humidity to realize the failure time prediction with different stresses using the early degradation data.
© 2019 Institute of Electrical Engineers of Japan. Published by John Wiley & Sons, Inc.

Keywords: tantalum capacitor; ordered clustering method; Davies-Bouldin index (DBI); degradation trend analysis

Received 3 July 2019; Revised 8 October 2019

1. Introduction

The tantalum capacitor is widely used in many fields, such as military, aerospace, and medical fields [1–3]. The performance of the tantalum capacitor directly influences the safe running of the system. Clustering method and degradation analysis can help to estimate the real-time performance to realize early warnings [4,5].

The influence of temperature on performance degradation of the tantalum capacitor has been studied in recent years. Li Bo, *et al.* [6] researched the degradation trend of capacitance (C) and dissipation factor (DF) of the tantalum capacitor from using temperatures of 25–205 °C. The experimental results showed that the capacitance C was approximately linear to the temperature and $\Delta C/C < 12\%$, and the DF increased with fluctuation in the degradation process. Dehbi, *et al.* [7] found that the capacitance changed little for 1000 h at 25, 85, and 125 °C, while the change at 150 °C was 2–3 times that at 25 °C. Deloffre, *et al.* [8] studied the relationship between capacitance and voltage of the tantalum capacitor in low-temperature stress of 5–300 k. The capacitance could increase linearly with increasing temperature. Peter *et al.* [9] proposed that the capacitance and dissipation factors of a tantalum capacitor with MnO_2 compared to those with polymer have different degradation degrees at 95 °C and 70% relative humidity (RH).

The performance of the tantalum capacitor is subject to temperature and humidity in practice. According to the degradation characteristics of the degradation parameters, such as capacitance and DF in our degradation test with different temperature and humidity, the clustering method could be used to distinguish different degradation regimes to complete the degradation trend analysis [10–12]. In Ref. [12], based on the ordered clustering model, the optimization cluster number of the temperature error of numerical control machine tools was obtained, and the prediction model was established.

In this paper, the degradation experiment of a tantalum capacitor with temperature and humidity is developed. Based on the degradation parameters of capacitance and dissipation factor, the performance mechanisms in different regimes are studied, and the sequential cluster algorithm is used. The optimization cluster number is determined by the natural property and the change rate of error function slope. The Davies-Bouldin Index (DBI) is used to estimate the cluster result. In a stable degradation regime, the degradation trend is analyzed to obtain the failure time according to the earlier data.

2. Degradation Experiment Design

The chip tantalum capacitor with polymer-PEDOT in the cathode is considered the research object, as shown in Fig. 1. The rated voltage and capacitance are 6.3 V and 330 μF, respectively. The failure criterion is as follows: capacitance decreases to below 264 μF or exceeds 396 μF (a deviation of ±20%); DF increases to above 10%.

The schematic representation of experiment setup in the body and the caption in Fig. 2 [9]. The Agilent N6702A is used as a DC source with 6.3 V and is switched by Agilent 34980A. Agilent 4263B LCR is used to measure the capacitance and dissipation factor. The samples are included in ESPEC PRA-3AP. The samples are connected in series with a 10 KΩ resistor.

Sixteen samples were tested at 95 °C and 70% RH. Variable time regime measurement is adopted to acquire the data with the same humidity and a temperature decrease to 25 °C, as shown in Figs 3 and 4, respectively. Then, each capacitor is fully discharged through a 5 KΩ resistor.

[a] Correspondence to: Jingying Zhao. E-mail: zhao_team@163.com

State Key Laboratory of Reliability and Intelligence of Electrical Equipment, Hebei University of Technology, Guangrong Avenue 8, Hongqiao District, Tianjin 300130, China

© 2019 Institute of Electrical Engineers of Japan. Published by John Wiley & Sons, Inc.

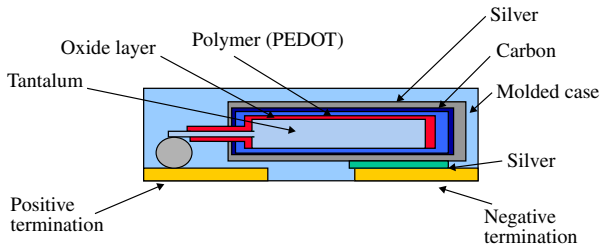

Fig. 1. Physical structure of tantalum capacitor

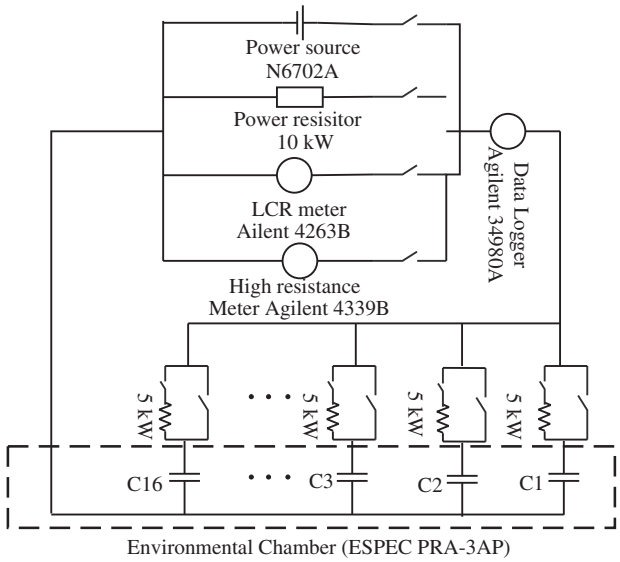

Fig. 2. Schematic representation of experiment setup

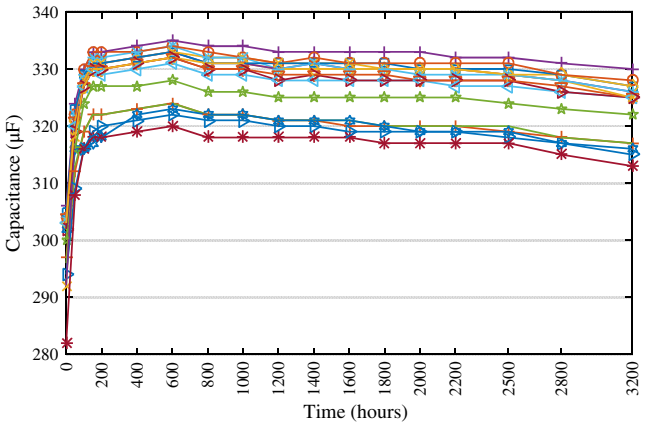

Fig. 3. Capacitance at 95 °C and 70% RH

3. Clustering Algorithm for Performance Degradation Trend

3.1. Degradation performance analysis With high temperature and high humidity, PEDOT expansion enlarges the effective contact area between cathode and dielectric material. Due to the different thermal expansion rates between the lead and the epoxy encapsulation layer, a small gap is formed [13], through which water quickly diffuses into the capacitor interior. In addition, water, Ta, and PEDOT form many tiny capacitors [14]. So, the capacitance increases rapidly before the moisture is saturated in Fig. 3.

Ref. [15] shows that mechanical stress has little effect on capacitance. From $C = \frac{\varepsilon_0 S}{d}$, the capacity degradation is caused by a decrease of dielectric constant.

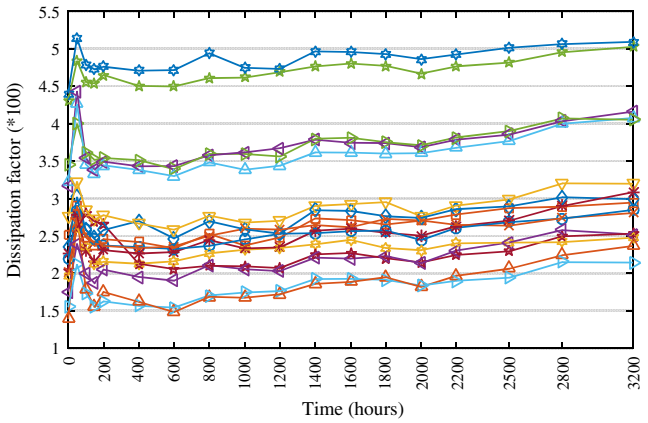

Fig. 4. Dissipation factor at 95 °C and 70% RH

DF tanδ is the tangent of a complementary angle of the phase difference between the AC voltage applied and the internal current flowing, which shows the dielectric insulation of the tantalum capacitor. It is determined by [16]

$$\tan\delta = \frac{ESR}{X_C} = \frac{ESR}{\omega C} \tag{1}$$

where ESR is equivalent series resistance, and X_c, C, and ω are equivalent reactance, capacitance, and working frequency, respectively.

In Fig. 4, PEDOT with water reduces the conductivity of the cathode and increases ESR [11] to make the DF increase quickly. With moisture saturation, ESR increases slowly, and capacitance increases quickly to result in the decrease of the DF. In the later stable degradation regime, the DF increases slowly.

3.2. One-step ordered clustering method The degradation mechanism of tantalum capacitor is different in different degradation regimes. The existing literature mainly analyzed the degradation performance with temperature and humidity and rarely mentioned the clustering method.

The degradation data has monotonous and nonlinear characteristics in different regimes. So, an ordered clustering model can be used to more accurately distinguish the different degradation regimes.

For the ordered data of degradation parameters, a Fisher algorithm is introduced. The basic principle is as folllows: First, n samples to be clustered are regarded as one cluster. Then, this cluster is divided into the required k clusters according to the principle of minimizing the deviation square sum of intracluster and maximizing the deviation square sum of intercluster. Assume that x_1, x_2, $\cdots$, x_p, $\cdots$, x_m are measurement points of the degradation parameters of n samples. The sequential cluster matrix is equal to

$$X = \begin{bmatrix} x_{11} & x_{12} & \cdots & x_{1m} \\ x_{21} & x_{22} & \cdots & x_{2m} \\ \vdots & \vdots & \vdots & \vdots \\ x_{n1} & x_{n2} & \cdots & x_{nm} \end{bmatrix} \tag{2}$$

where m = 1, 2, $\cdots$, 18; n = 1, 2, $\cdots$, 16.

In order to simplify the calculation, the degradation data are standardized using (3).

$$w_{ij} = \frac{x_{ij} - \min\limits_{1\le j\le m}\{x_{ij}\}}{\max\limits_{1\le j\le m}\{x_{ij}\} - \min\limits_{1\le j\le m}\{x_{ij}\}} \tag{3}$$

where w_{ij} is degradation parameter at j measurement point of i sample. i = 1, 2, $\cdots$, n; j = 1, 2, $\cdots$, m.

The standardized sequential cluster matrix is determined by

$$W = \begin{bmatrix} w_{11} & w_{12} & \cdots & w_{1m} \\ w_{21} & w_{22} & \cdots & w_{2m} \\ \vdots & \vdots & \vdots & \vdots \\ w_{n1} & w_{n2} & \cdots & w_{nm} \end{bmatrix} \tag{4}$$

3.3. Category diameter calculation Category diameter between the homogeneous clusters need to be minimized. Assume that $\{w_{\mathrm{pi}}, w_{p(i+1)}, \ldots, w_{\mathrm{j}}\}$ is a clustering subregime of the degradation parameter of sample p; then, the mean distance is equal to

$$\overline{w_{p\cdot ij}} = \frac{1}{j-i+1}\sum_{i=1}^{j} w_{pi} \tag{5}$$

where $1 \le i \le j \le m$.

Then, the category diameter of degradation parameters of n samples can be determined by

$$\mathrm{d}(i,j) = \sum_{p=1}^{n}\sum_{t=i}^{j}(w_{pt} - \overline{w_{p\cdot ij}})^2 \tag{6}$$

3.4. Error function determination The degradation trend is divided into k categories.

$$\{w_{j_1=1}, w_2, \cdots, w_{j_2-1}\}, \{w_{j_2}, w_{j_2+1}, \cdots, w_{j_3-1}\}, \cdots, \{w_{j_k}, w_{j_k+1}, \cdots, w_m\} \tag{7}$$

where $j_1 = 1 < j_2 < \cdots < j_{\mathrm{k}} < m$.

The error function $\widetilde{\delta}[p(m,k)]$ is

$$\widetilde{\delta}[p(m,k)] = \sum_{i=1}^{k} d(j_i, j_{i+1} - 1) \tag{8}$$

The smaller the error function$\widetilde{\delta}[p(m,k)]$, the smaller the intracluster difference. So, the minimum error function $\delta[p(m, k)]$ is determined by

$$\delta[p(m,k)] = \min\widetilde{\delta}[p(m,k)] \tag{9}$$

3.5. Clustering number optimization Clustering number optimization can be obtained by the inductive method of cluster algorithm.

$$\delta[p(m,2)] = \min_{2\le i\le m}\{d(1,j_{i-1}) + d(j_i,m)\} \tag{10}$$

$$\delta[p(m,k)] = \min_{k\le i\le m}\{d(j_{i-1},j_{k-1}) + d(j_i,m)\} \tag{11}$$

When $m = k$, it can be considered that there are two clusters according to (11): $\{1, 2, \cdots, j_i - 1\}$ and $\{j_i, j_{\mathrm{i}}+1, \cdots, m\}$; then, $\{1, 2, \cdots, j_i - 1\}$ is divided into $k-1$ clusters. The clustering optimization can be completed by j. The clustering results are shown in Tables I and II. The last measurement point of each cluster is taken as the division point.

4. Clustering Number Optimization of Degradation Parameter

4.1. Clustering number optimization method According to Tables I and II, the optimal cluster number is determined by the natural property and the relationship between error function and k, but this method is not accurate. Therefore, a new method is shown by the introduction of the change rate $\alpha(k)$ of the slope $\beta(k)$ of the error function $\delta[p(m, k)]$.

Table I. The clustering optimization of capacitance

Cluster	Error δ	Optimal clustering
1	0.896	1–18
2	0.1344	1,2–18
3	0.04	1,2,3–18
4	0.0241	1,2,3-16,17–18
⋮	⋮	⋮
17	0	1,2,3,4,5,6,7,8,9,10,11,12,13,14,15-16,17,18
18	0	1,2,3,4,5,6,7,8,9,10,11,12,13,14,15,16,17,18

Table II. The clustering optimization of dissipation factor

Cluster	Error δ	Optimal clustering
1	0.82	1–18
2	0.6505	1–15,16–18
3	0.2533	1,2,3–18
4	0.0881	1,2,3-9,10–18
⋮	⋮	⋮
17	0.0001	1,2,3,4,5,6,7,8,9,10,11-12,13,14,15,16,17,18
18	0	1,2,3,4,5,6,7,8,9,10,11,12,13,14,15,16,17,18

Table III. The two-step optimal clustering results of capacitance

Cluster	Error δ	Optimal clustering
1	2.4591	1–16
2	1.0617	1–7,8–16
3	0.6846	1–7,8-14,15–16
4	0.3525	1,2-7,8-14,15–16
⋮	⋮	⋮
14	0.0022	1,2-3,4,5,6–7, 8,9,10,11,12,13,14,15,16
15	0.0001	1,2-3,4,5,6,7,8,9,10, 11,12,13,14,15,16

$$\beta(k) = \delta[p(m,k+1)] - \delta[p(m,k)] \tag{12}$$

$$\alpha(k) = \left|\frac{\beta(k) - \beta(k-1)}{\beta(k) - \beta(k+1)}\right| \tag{13}$$

when $\alpha(k)$ is maximum, the optimal clustering number can be obtained as k. Considering natural properties of the samples, it may continue to classify by cluster algorithm.

4.2. Degradation regime division of capacitance In Table I, when $k = 2$, the maximum $\alpha(k)$ is 17.07 using (13), that is, capacitance can be divided into different regimes with 0–50, 50–100, and 100–3200 h. However, stable degradation state has not been reached at 100 h as seen in Fig. 3. According to the natural properties, a two-step clustering algorithm is introduced. The result is shown in Table III, representing 16 measured points during 100–3200 h.

In Table III, when $k = 2$, the maximum $\alpha(k)$ is 22.67 using (13), that is, different regimes with 100–1200 and 1200–3200 h are obtained. So, the capacitance degradation is divided into four regimes, as shown in Fig. 5.

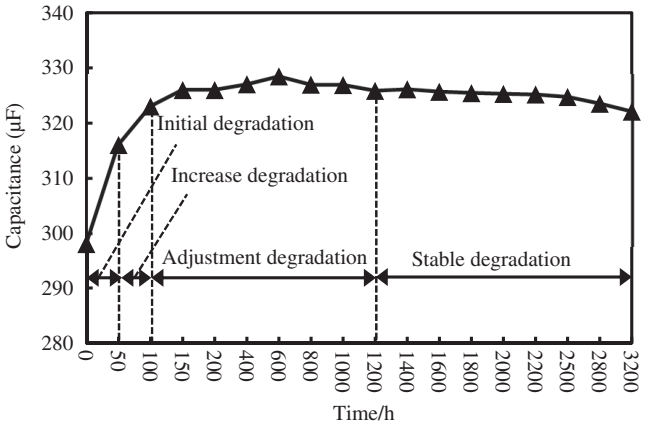

Fig. 5. Degradation regime division of capacitance at 95 °C and 70% RH

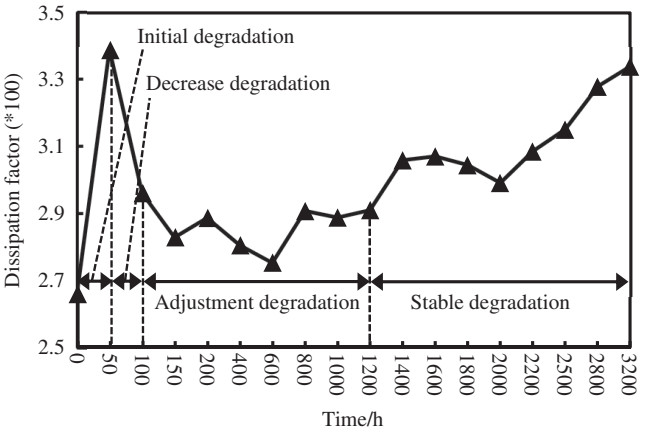

Fig. 6. Degradation regime division of dissipation factor at 95 °C and 70% RH

1 Initial degradation regime (0 to 50 h): The average of capacitance is 299 μF, which is about 9.4% less than nominal capacitance. The average of the capacitance sharply increases to 18 μF, which is caused by the rapid diffusion of water before moisture is not in balance.
2 Increase degradation regime (50 to 100 h): The internal moisture of the capacitor is gradually saturated. The average increase of capacitance is only 7 μF.
3 Adjustment degradation regime (100 to 1200 h): Water of the capacitor is saturated. The capacitance rises to rated value. The capacitance reached at the rated capacitance.
4 Stable degradation regime (1200 to 3200 h): With water saturation, the capacitance slowly decreases by 4 μF in 2000 h. The degradation of the capacitance is mainly caused by the decrease of the dielectric constant at high temperature.

4.3. Degradation regime division of dissipation factor

In Table II, when $k = 4$, the maximum $\alpha(k)$ is 41.83 using (13). Degradation regime division is completed by the one-step clustering method. Different regimes of the DF with 0–50, 50–100, 100–1200, and 1200–3200 h are obtained, as shown in Fig. 6.

1 Initial degradation regime (0 to 50 h): DF increases drastically by 0.73% because water reduces the conductivity of the cathode, leading to an increase in ESR.
2 Decrease degradation regime (50 to 100 h): DF decreases drastically by 0.56% and has a peak at 50 h because the capacitance increases rapidly during 50 h, and the DF is inversely proportional to it.
3 Adjustment degradation regime (100 to 1200 h): There is a balance between the internal water and the external water in this regime. DF change is not obvious.
4 Stable degradation regime (1200 to 3200 h): The increasing ESR of Ta_2O_5 results in the slow increase of the dissipation factor.

The regime division of the DF based on the one-step clustering algorithm is consistent with the degradation trend in Fig. 3, the degradation mechanism, and the regime division of the capacitance.

4.4. Clustering effectiveness verification

DBI [17] is the average value of the maximum ratio of intracluster distances in any two clusters to the distance between the two clusters. DBI refers to the similarity degree of the data in the same cluster and the deviation degree among clusters. It can be used to verify the effectiveness of the clustering method. DBI is equal to

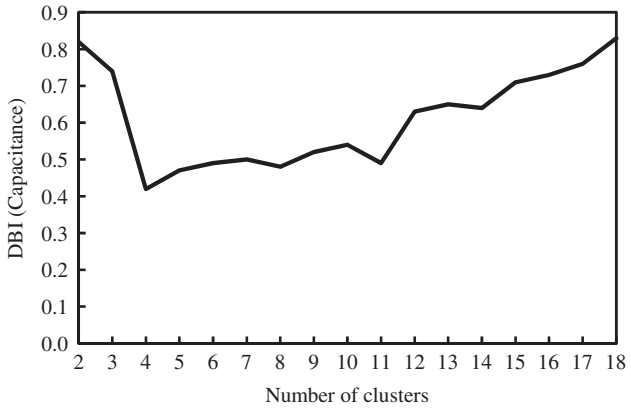

Fig. 7. Davies-Bouldin Index (DBI) of capacitance

$$DBI = \frac{1}{N}\sum_{i=1}^{N}\max_{j\neq i}\left(\frac{S_i + S_j}{d(c_i, c_j)}\right) \tag{14}$$

where S_i and S_j are the average intracluster distance, representing the deviation degree of degradation data in one cluster; $d(c_i, c_j)$ is the distance between cluster i and cluster j; and N is the clustering number.

The smaller the DBI, the smaller the distance within data in one cluster and the larger the distance between different clusters. The DBIs of capacitance and DF are shown in Figs 7 and 8, respectively. DBIs are only 0.42 for capacitance and 0.35 for dissipation factor.

5. Ordered Clustering Algorithm Verification

In order to verify the effectivity of the ordered clustering algorithm of degradation performance of tantalum capacitor and if the division of regimes is consistent with the degradation mechanism, with 85 °C and 85% RH, five samples of the same type are measured. The results are shown in Figs 9 and 10. The calculations of the clustering optimization are shown in Table IV by one-step or two-step clustering algorithm.

In Table IV, the degradation trend of capacitance can be divided into three regimes: 0–100, 100–1000, and 1000–3000 h, and the degradation trend of DF can be divided into four regimes: 0–50, 50–150, 150–900, and 900–3000 h. DBIs are 0.54 and 0.39, respectively. The stable degradation regime can start at 1000 h.

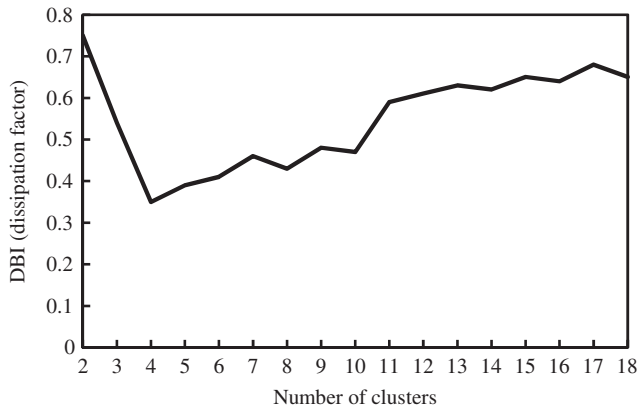

Fig. 8. Davies-Bouldin Index (DBI) of dissipation factor

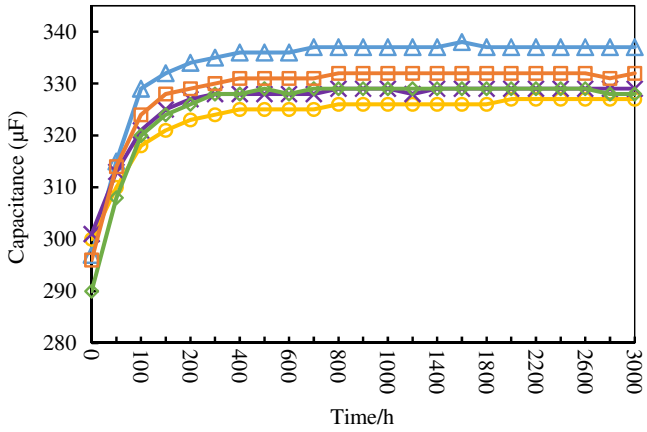

Fig. 9. Degradation of capacitance with 85 °C and 85% RH

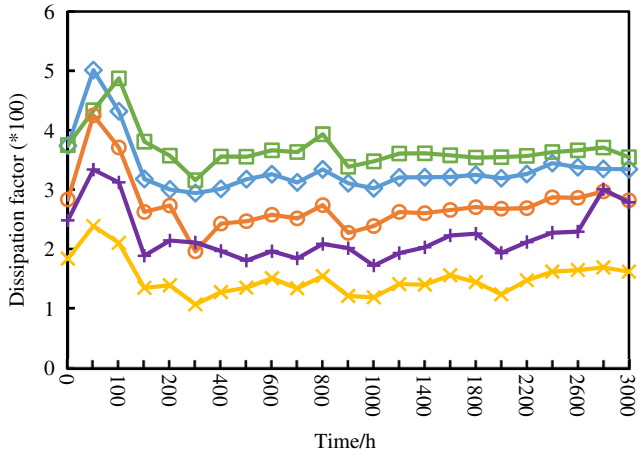

Fig. 10. Degradation of dissipation factor with 85 °C and 85% RH

6. Degradation Trend Analysis

6.1. Degradation fitting analysis Different degradation parameters can reflect the performance change of the tantalum capacitor. The degradation fitting function can fit the degradation trend well to provide an effective means for performance monitoring.

The steps to acquire the degradation fitting functions are as follows:

1 According to the ordered clustering analysis, with 95 °C and 70% RH, the stable degradation regime starts at 1200 h.

Table IV. The optimization cluster of capacitance and dissipation factor with 85 °C and 85% RH

Parameter	Step of cluster	$\alpha(k)$	Numbers of cluster	Optimal clustering
Capacitance	One-step	20.01	2	1–2,3–23
	Two-step	7.69	2	1–10,11–21
Dissipation factor	One-step	117.63	4	1,2-3,4-11,12–23

2 For the nonlinear and increasing trend of capacitance and dissipation factor, degradation fitting functions with confidence levels of 95% are chosen as

$$f(t) = p_1 t^2 + p_2 t + c$$
$$f(t) = p_1 t^3 + p_2 t^2 + p_3 t + c$$
$$f(t) = p_1 t^{p2} + c \tag{15}$$

where $f(t)$ is capacitance or dissipation factor; p_1, p_2, p_3, and c are the coefficient of models.

The variations of capacitance and DF differ greatly from that of time by orders of magnitude. In order to improve the fitting accuracy, t in (15) is normalized by a mean value of 2078 and a SD of 662 according to the time in the stable degradation regime, that is, $z = \frac{t-2078}{662}$, and then, $f(t)$ can be calculated by inverse transformation.

3 The least-square method is introduced to fit the degenerate trends, determine the coefficients in (15), and minimize R in (16)

$$R = \sum_{i=1}^{n} (y_i - f(t_i))^2 \tag{16}$$

where y_i is the actual value of the degradation data, $f(t_i)$ is fitting value of degradation data, n is 9 in the stable regime. The fitting result and function coefficients are shown in Table V.

4 In Table V, according to sum of squares due to error and R-square, the cubic polynomial is more suitable as a degradation fitting function of capacitance and dissipation factor. The fitting curves are shown in Figs 10, 11 and 12. The average error of capacitance and DF are 5.4 and 6.7%, respectively. In practice, the self-healing characteristics of tantalum capacitor causes the degradation data to fluctuate.

5 With 85 °C and 85% RH, degradation regime division of capacitance is completed by the two-step clustering method with 0–50, 50–150, 150–1000, and 1000–3000 h and that of DF by one-step clustering method with 0–50, 50–200, 200—1000, and 1000–3000 h. The stable regime starts at 1000 h. The fitting degradation functions of capacitance and DF are as follows (It is normalized by a mean value of 2000 and a SD of 663):

$$C = -0.05102t^3 - 0.1128t^2 + 0.1067t + 330.8 \tag{17}$$

$$DF = 0.03315t^3 - 0.004996t^2 + 0.08801t + 2.649 \tag{18}$$

The fitting curves of capacitance degradation and DF degradation are shown in Figs. 13 and 14, and the average errors of capacitance and DF are11.2 and 7.3%, respectively. The cubic polynomial method can be used as the degradation fitting function with different stresses.

Table V. Fitting result and function coefficients of degradation performance with 95 °C and 70% RH

Parameters	Function	Result		Function coefficient			
		R-square	SSE	c	p_1	p_2	p_3
Capacitance	Quadratic polynomial	0.9109	1.148	325.3	−0.4132	−1.022	
	Cubic polynomial	0.9541	0.5917	325.2	−0.368	−0.2219	−0.4275
	Power function	0.9299	0.9039	325.9	−4.09E-15	4.269	
Dissipation factor	Quadratic polynomial	0.8588	0.0205	3.079	0.02749	0.1137	
	Cubic polynomial	0.8646	0.0197	3.082	0.01434	0.02003	0.09053
	Power function	0.8602	0.0203	2.947	2.48E-10	2.629	

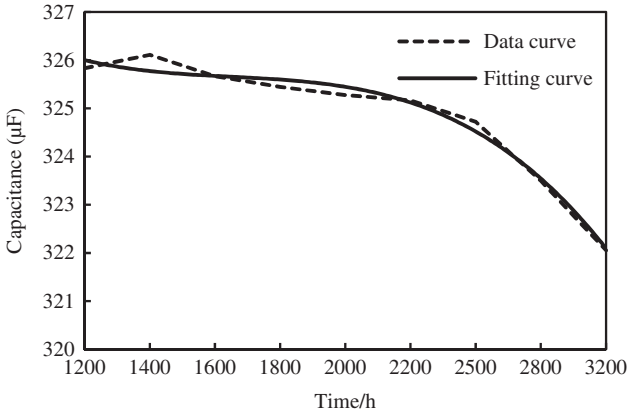

Fig. 11. Degradation fitting curve of capacitance with 95 °C and 70% RH

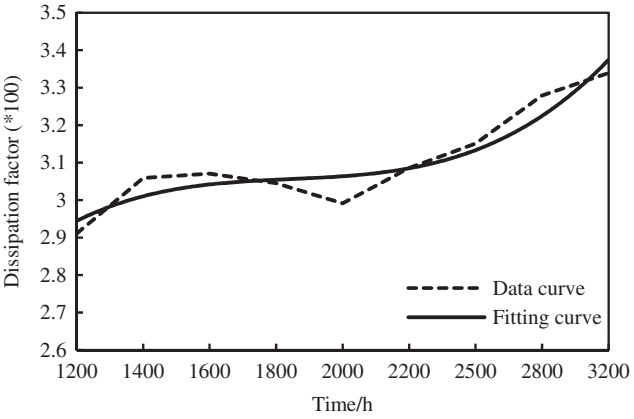

Fig. 12. Degradation fitting curve of dissipation factor with 95 °C and 70% RH

6.2. Degradation prediction method According to degradation fitting analysis, in order to achieve a degradation prediction life with different stresses, another test is completed. With 110 °C and 85% RH, five samples of the same type are measured. The results are shown in Figs 15 and 16.

Degradation regime division of capacitance is completed by the two-step clustering method with 0–12, 12–25, 25–200, and 200–1000 h and that of DF by one-step ordered clustering method with 0–75, 75–200, and 200–1000 h. The stable degradation regime starts at 200 h and the degradation fitting functions of capacitance and DF are obtained (it is normalized by a mean value of 600 and SD of 273):

$$C = -0.1279t^3 - 0.1071t^2 - 0.1821t + 333.1 \quad (19)$$

$$DF = 0.1739t^3 + 0.06344t^2 + 0.4461t + 3.833 \quad (20)$$

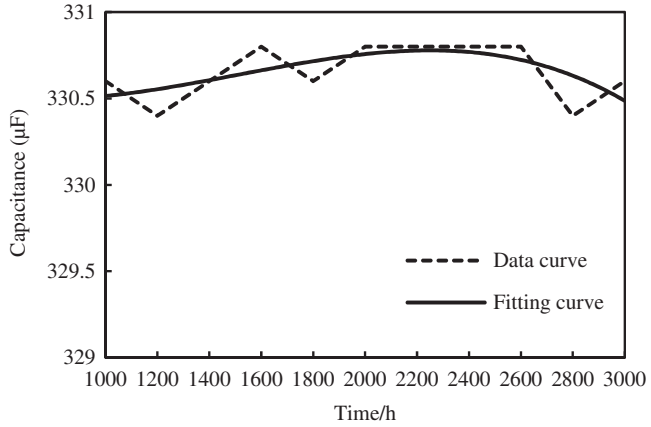

Fig. 13. Capacitance degradation fitting curve with 85 °C and 85% RH

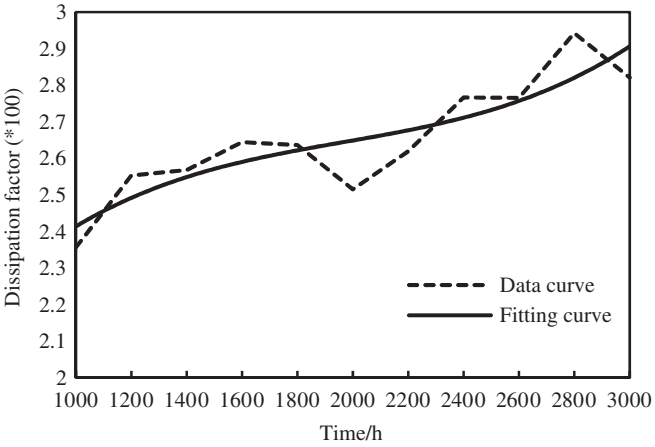

Fig. 14. Degradation fitting curve of dissipation factor with 85 °C and 85% RH

According to the failure criterion shown in Section 2 and the degradation fitting functions with 95 °C and 70% RH, 85 °C and 85% RH, and 110°C and 85% RH, the prediction lives are given in Table VI.

According to Table VI, the relationships between the prediction life and the stress are obtained, as shown in Figs 17 and 18.

With different temperature and humidity, the degradation of the DF is more obvious than that of capacitance. So, the DF can be used to predict the life of the tantalum capacitor to provide early warning for the failure and replacement of this capacitor. With 110 °C and 85% RH, DF of the sample, represented by circles in Fig. 16, rises sharply by 43.4% at 1200 h, and the sample fails according to the failure criterion. Compared with the predicted life in Table VI, the error is 14%.

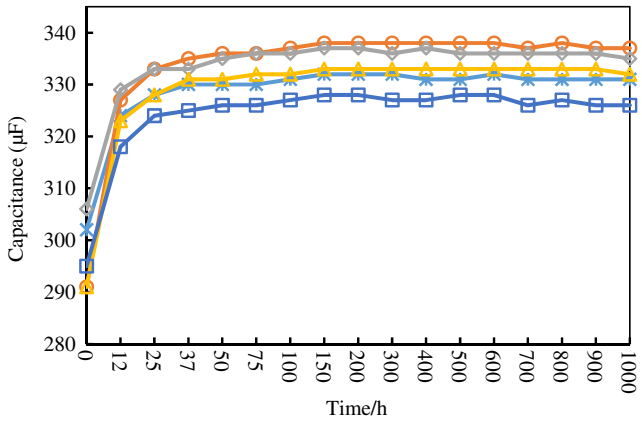

Fig. 15. Capacitance with 110 °C and 85% RH

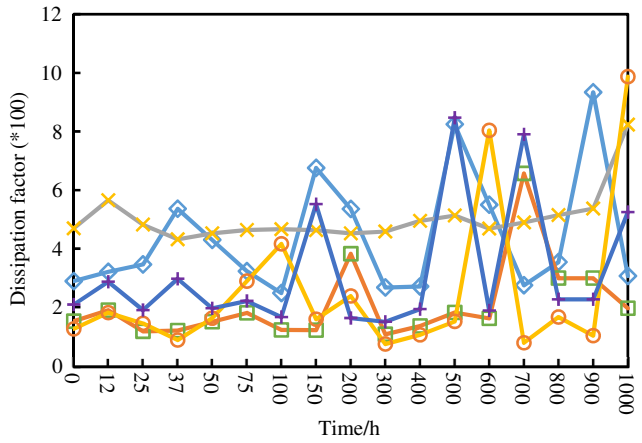

Fig. 16. Dissipation factor with 110 °C and 85% RH

Table VI. Prediction life with different stresses

Life (h)	Parameter	
Stress	Capacitance	Dissipation factor
95 °C and 70% RH	8274	6812
85 °C and 85% RH	13 917	5883
110 °C and 85%RH	4282	1399

7. Conclusion

1 This paper develops an ordered clustering method and degradation trend analysis for performance degradation of the tantalum capacitor. The main conclusions are as follows:

2 Capacitance and DF of tantalum capacitor are chosen as the degradation parameters, and a degradation experiment with different temperature and humidity is designed. According to the degradation data, the failure mechanisms are analyzed.

3 A two-step ordered clustering method for degradation trend of the capacitance and a one-step ordered clustering method for degradation trend of the DF are introduced. Combining the natural properties and the change rate of the slope of the error function, the optimal clustering number is determined with 95 °C and 70% RH, which is estimated by DBI as 0.42 for capacitance and 0.35 for dissipation factor. In addition, the ordered clustering method was verified using other data with other stresses.

4 According to the ordered clustering results, in a stable degradation regime, the degradation fitting functions are established by cubic polynomial function. Degradation fitting analysis with 95 °C and 70% RH is completed, and the fitting method is verified by other degradation data with different temperature and humidity. When the fitting results and experimental results are compared, the maximum error was less than 8%. Using degradation trend analysis with 95 °C and 70% RH, 85 °C and 85% RH, and 110°C and 85% RH, the degradation prediction is completed to find the relationship between prediction life and different temperature and humidity, which is obtained to realize early warning and product replacement through the use of early degradation data.

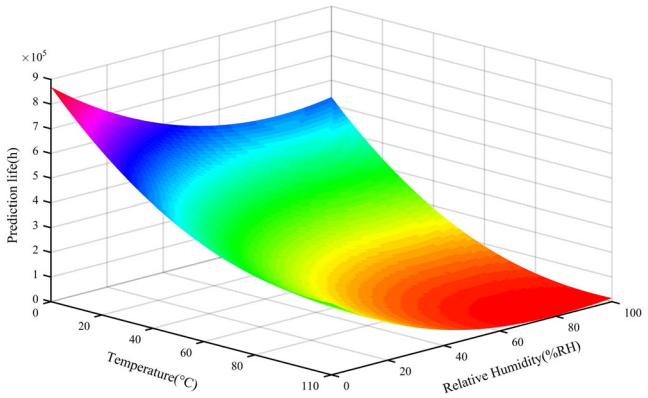

Fig. 17. Relationship between prediction life and different temperature and humidity according to capacitance

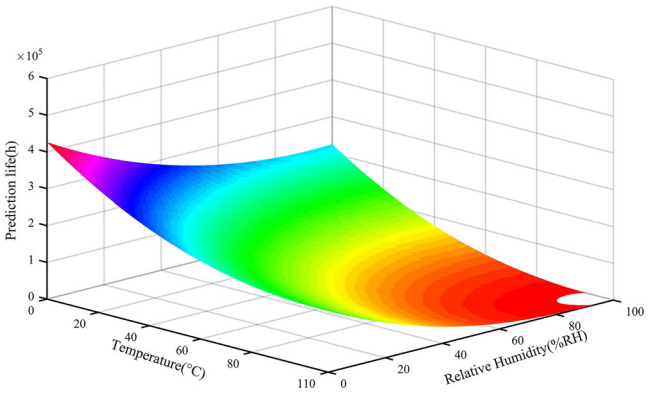

Fig. 18. Relationship between prediction life and different temperature and humidity according to dissipation factor

Acknowledgments

We thank the Center for Advanced Life Cycle Engineering (CALCE) at the University of Maryland and China Scholarship Council (CSC) for supporting the research activities.

References

(1) Abuetwirat I, Liedermann K. Dielectric properties of thin tantalum oxide layers at solid tantalum capacitors. *International Conference on Computer Information Systems & Industrial Applications* 2015; **18**:889–891.

(2) Teverovsky A. Degradation of leakage currents and reliability prediction for tantalum capacitors. In *Annual Reliability and Maintainability Symposium (RAMS)*. IEEE: Piscataway, NJ; 2016; 1–7.

(3) Niu B, Chen ZY, Xu ZM. Method for recycling tantalum from waste tantalum capacitors by chloride metallurgy. *ACS Sustainable Chemistry & Engineering* 2017; **5**(2):1376–1381.

(4) Virkki J, Frisk L, Heino P and Kuusiluoma S. Enhanced moisture stress test method for capacitors. *Iciea: 2009 4th Ieee Conference on*

Industrial Electronics And Applications, vols. 1–6, pp. 3992–3995, 2009.
(5) Yoon JS, Kim BI. Characteristics and production of tantalum powders for solid-electrolyte capacitors. *Journal of Power Sources* 2007; **164**(2):959–963.
(6) Bo L, Ya Z, Jian-jun X, Shi-zhong L. Parameters variation mechanism of solid electrolytic tantalum capacitors in very high temperatures. *Transactions of Beijing Institute of Technology* 2009; **29**(10):921–923.
(7) Dehbi A, Wondrak W, Ousten Y, Danto Y. High temperature reliability testing of aluminum and tantalum electrolytic capacitors. *Microelectronics Reliability* 2002; **42**(6):835–840.
(8) Deloffre E, Montes L, Ghibaudo G, Bruyere S, Blonkowski S, Becu S, Gros-Jean M, Cremer S. Electrical properties in low temperature range (5 K-300 K) of tantalum oxide dielectric MIM capacitors. *Microelectronics Reliability* 2005; **45**(5–6):925–928.
(9) A. Peter, M. H. Azarian and M. Pecht: Reliability of manganese dioxide and conductive polymer tantalum capacitors under temperature humidity Bias testing, **2015**, 1, pp.000713–000719 (2015)
(10) Ban MF, Yu JL, Ge J. Procedural modeling for charging load of electric buses cluster based on battery swapping mode. In *Intelligent Computing in Smart Grid and Electrical Vehicles, vol. 463*. Springer: Berlin, Heidelberg; 2014; 505–516.
(11) Wang YH, Zhang YW, Wan P, Zhang SC, Yang J. A Spectrum sensing method based on empirical mode decomposition and K-means clustering algorithm. *Wireless Communications and Mobile Computing* 2018; **6104502**:1–6104502:10.
(12) Gao F, Liu J, Yang X, Li Y, Yang Y. Study on optimization of thermal key points for machine tools based on Fisher optimal segmentation method. *Chinese Journal of Scientific Instrument* 2013; **34**(5):1070–1075.
(13) Sun ZW, Deng CZ, Tsai KC. Performance of mixed ruthenium and tantalum oxide packaged ultracapacitors. *Proceedings Of the Symposium on Electrochemical Capacitors Ii* 1997; **96**(25):43–52.
(14) Teverovsky AA. Effect of moisture on characteristics of surface mount solid tantalum capacitors. In *Carts-Conference*. Components Technology Institute Inc, 2003.
(15) Teverovsky A. Effect of mechanical stresses on characteristics of chip tantalum capacitors. *IEEE Transactions on Device and Materials Reliability* 2007; **7**(3):399–406.
(16) Gournay P. Capacitance and dissipation factor measurements under high voltage at BNM-LCIE. *2000 Conference on Precision Electromagnetic Measurements Digest*, pp. 419–420, 2000.
(17) Davies DL, Bouldin DW. A cluster separation measure. *IEEE Transactions on Pattern Analysis and Machine Intelligence* 1979; **PAMI-1**(2):224–227.

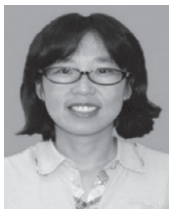

Jingying Zhao (Non-member) received M.S. and Ph.D. degrees from the school of Electrical Engineering, Hebei University of Technology, Tianjin, China, in 2000 and 2004, respectively. She is currently a professor with the School of Electrical Engineering, Hebei University of Technology, Tianjin, China. Her research interests are electrical reliability and detection technology and wireless power transfer.

Jianmeng Liu (Non-member) received a B.S. degree from the School of Electrical Engineering and Automation, Shijiazhuang University, Hebei, China, in 2017. He is currently studying for an M.S. degree at the School of Electrical Engineering, Hebei University of Technology, Tianjin, China. His research focuses on the tantalum capacitor.